



**AUTHOR(S):**

**TITLE:**

**YEAR:**

**Publisher citation:**

**OpenAIR citation:**

**Publisher copyright statement:**

This is the \_\_\_\_\_ version of an article originally published by \_\_\_\_\_  
in \_\_\_\_\_  
(ISSN \_\_\_\_\_; eISSN \_\_\_\_\_).

**OpenAIR takedown statement:**

Section 6 of the "Repository policy for OpenAIR @ RGU" (available from <http://www.rgu.ac.uk/staff-and-current-students/library/library-policies/repository-policies>) provides guidance on the criteria under which RGU will consider withdrawing material from OpenAIR. If you believe that this item is subject to any of these criteria, or for any other reason should not be held on OpenAIR, then please contact [openair-help@rgu.ac.uk](mailto:openair-help@rgu.ac.uk) with the details of the item and the nature of your complaint.

This publication is distributed under a CC \_\_\_\_\_ license.

\_\_\_\_\_

## **Abstract**

In clastic reservoir oilfields where chemical inhibitors are used for mitigating scale problems, understanding the interaction between chemical inhibitor species and fabrics of reservoir sands is very crucial in the evaluation of rock geomechanical properties for sand production related field optimization. The current oil industry approach to geomechanical evaluation of reservoir formations that have experienced significant application of chemical inhibitors does not in any way take into consideration any potential effects of the chemical inhibitors on the reservoir formation fabrics. It is more often than not assumed that the interaction between the chemical inhibitor species and the sand materials is of no geomechanical significance. Laboratory experiments were performed on Clashach cores representing clastic reservoir formation analogues to investigate the nature of the interaction between a chemical scale inhibitor and reservoir formation. The experimental results show that the interaction between chemical inhibitor and reservoir sand materials led to the weakening of sand fabrics, triggering sand failure and release into the flow streams. The results also show that the inhibitor-formation interaction is of great significance in formation rock geomechanical characterization for failure analysis optimization. Based on the experimental results conceptual physico-chemical failure models are proposed for analyzing and describing the inhibitor-formation interaction

## **Introduction**

Evaluation of geomechanical properties of reservoir formation is a key requirement in sand production related field optimization [Oluyemi et al 2010]. In reservoir formations, which have had substantial contact with scale inhibitors and other related oilfield chemicals via field chemical injection programme, geomechanical evaluation

of the rock is often done without any consideration for the likely effects of these chemicals on the formation strength [Oluyemi 2007]. A Previous work [Engebretson et al 1997] has investigated the effect of chemicals such as dodecyltrimethyl ammonium bromide (DTAB), polyethylene oxide (PEO) and aluminium chloride ( $\text{AlCl}_3$ ) on the strength of sandstone to establish fundamental knowledge which can be used in the optimization of chemically assisted fracturing. However, the scope of the work was not extended to the possible dynamic effects on the sand strength reduction and sand failure. Besides, the chemicals used in the study have totally different chemistries from the common oil industry scale inhibitors' chemistries.

In this current work, we investigate, under dynamic conditions, any likely effects of scale inhibitors on the geomechanical strength and sand production potentials of “soft” clashach rock analogous to unconsolidated reservoir rock.

## **Experimental design and implementation**

### ***Materials and Equipment***

Two identical cores – labeled Core A and Core B - were sourced from the same Clashach sandstone block and used as substrates for the experimental work. Clashach sandstone is analogous to a reservoir sand formation with relatively low clay content. The dimensions of the two cores are shown in Table 1. The saturating and injection fluid was prepared by diluting a number of various salts in de-ionised filtered water. The salts used and their concentration are given in Table 2. The brine was filtered through a 45um filter paper before every use. The use of filtered brine ensured no extraneous fines were introduced to the cores and helped to stabilize any clay minerals that might already be present in the cores. A stock of 5% phosphonate scale

inhibitor (PTEMP) solution was prepared by diluting 12.50 g of the SI in 250 ml of brine.

The following pieces of equipment were used in the experimental work:

- Coreflood rig with a pressure rating of 100 bars absolute line pressure and 50 psi differential pressure
- Hassler-type core-holder with a pressure rating of 5000 psi
- Malvern Mastersizer 2000 – for grain size distribution measurement
- Vacuum filter pump with maximum pressure rating of 20 bars
- Programmable pump with a working pressure of 100 bars

## **Procedures**

The following procedures implemented in three stages were used to carry out the experimental work.

### ***Stage 1 – Static saturation of Clashach cores***

The two identical cores were put in a beaker and brine poured into the beaker well enough to cover the two cores. The cores were left for a week in the brine to be fully saturated. A week was considered long enough for complete static saturation of the cores. At the end of one week, the cores were removed from the brine effluent. The effluent was stirred using a magnetic stirrer and samples of the effluent taken while being stirred. The samples of original brine were also taken. The grain size distribution of the original brine and effluent samples were measured using Malvern Mastersizer 2000, the rationale being to compare the pre and post core saturation brine grain size profiles.

## ***Stage 2 – Dynamic saturation of Clashach cores and key petrophysical properties measurement***

Immediately after removing the two cores from the brine in stage 1, each was set in a separate Hassler-type core holder which was then attached to a separate core flood rig. The process design flow diagram of the coreflood rig set-up is shown in Figure 1.

The cores were saturated separately by flowing brine through them for 6 hours at a flow rate of 1 ml/min. Low flow rate ensured that the interstitial velocity of flow was laminar enough to keep fines from clay minerals stabilized whilst long saturation time ensured that the cores were fully saturated. The porosities of the two cores were measured using lithium tracer techniques. The procedure for implementing this porosity measurement technique can be found elsewhere in the literature [Oluyemi et al 2009; Graham et al 2009]. Lithium is an inert metal; the use of Lithium tracer technique therefore ensured that there was no interaction – physical or chemical – between the cores and the lithium fluid. The permeabilities of the two cores were also measured using flow rates of 1ml/min, 4ml/min, 3ml/min, 2ml/min and 1ml/min in sequence. Effluent samples were collected from each flow system (i.e. cores 1 and 2) during the highest flow rate regime and their grain size distributions were measured using Malvern Mastersizer 2000.

## ***Stage 3 – Scale Inhibitor injection***

13 ml of scale inhibitor stock just enough to fully saturate the pore volume of either of the cores was Injected into one of the cores – core A - at a flow rate of 0.25ml/min. Again, low flow rate was used in order to eliminate any possible high flow-rate effects. The core-holders inlet and outlet valves were then shut down and the cores left overnight to allow for a longer interaction time between the core and SI. Brine

was continuously injected into the second core – core B – overnight. The scale inhibitor was then flushed out of core A using the filtered brine at a flow rate of 0.25ml/min. Effluent samples were collected from inhibitor flowback from core A and brine injection from core B. The grain size distributions of the effluent samples were measured using Malvern Mastersizer 2000

## **Discussion of results**

### ***Static saturation of Clashach cores***

Figure 2 compares the grain size distributions of both the original brine and effluent samples obtained during the static saturation of cores A and B. The grain size distribution profiles obtained for the three different fluids show similar shape and pattern. More importantly, their  $d_{10}$ ,  $d_{50}$  and  $d_{90}$  values were close. This is an indication that the brine had no detrimental physical or chemical effects on the grain fabric which could have caused the deterioration of grain-to-grain binding and subsequent grain release and appearance in the brine effluents. This outcome is consistent with the outcome of the visual inspection of the two brines which showed that there were no visible particles in the “saturating” beaker as a result of brine-core interaction. It can also be seen in Figure 2 that the smallest particle size found in the brine and the effluents was around 44 microns. This is consistent with the fact that the original brine was filtered through a 45 microns filter paper before use.

### ***Dynamic saturation of Clashach cores and key petrophysical properties measurement***

Figure 3 shows the Li tracer profiles obtained from the pore volume and porosity measurements. Pore volume and porosity values calculated from the profiles for both cores are shown in Table 3. The results show striking similarities in the pore volume and porosity properties of the two cores. Similarly, Figure 4 shows the pressure profiles obtained from the permeability measurements for both cores. The calculated permeability values from the pressure profiles for both cores are shown in Table 4. The values obtained for both cores are also strikingly similar, further showing that differences in the two cores, if any, were not significant.

Figure 5 compares the grain size distributions of both the original brine and effluent samples obtained during the dynamic saturation of both cores. The grain size distribution profiles obtained for the three fluids also show similar shape and pattern, with similarly close  $d_{10}$ ,  $d_{50}$  and  $d_{90}$  values. In a similar manner, this indicates that neither the brine nor the dynamic flow condition had any detrimental physical or chemical effects on the grain fabric which could have caused the deterioration of grain-to-grain binding and subsequent grain release and appearance in the flow stream.

### ***Scale inhibitor injection***

Figure 6 shows the grain size distribution profiles of both inhibitor flowback (core A) and brine injection (core B) effluents. The figure shows no significant difference in shape and value between the grain size distribution profiles of brine injection effluent and the original brine. However, a significant difference in value is seen in the grain size distribution profiles obtained for the inhibitor flowback effluent and the original

brine. The  $d_{10}$ ,  $d_{50}$  and  $d_{90}$  of the inhibitor flowback effluents have increased respectively from between 20-22 microns, 10-12 microns and 0.25 microns to 38 microns, 24 microns and 1 micron. This is a clear indication that substantial additional particles were introduced into the flow stream from core A materials during the SI injection and saturation stage. The inhibitor interaction with the core materials may have led to the weakening of the core grain fabrics leading to the deterioration of grain-to-grain binding and subsequent release and movement of sand grains

### **Conceptual physico-chemical models**

The major stabilizing factors of unconsolidated sands include strength derived from capillary bonding [Han et al 2002] and the strength due to cementitious materials and mechanical attributes of sand [Han et al 2002; Han & Dusseault 2002; Papamichos et al 1997]. Capillary bonding results from interfacial tension between two immiscible fluid phases in a porous medium which furnishes a cohesive strength. The cohesive strength helps to keep the sand grains together even when they have already failed. [Han & Dusseault 2002; Papamichos et al 1997]

The laboratory results obtained from this study can therefore be explained using the following conceptual physico-chemical models:

- Chemical reaction between the SI species and the formation water (brine) may lead to formation and deposition of new materials in the formation pore throats, blocking the paths of the pore throats. During production, as simulated by the inhibitor flowback stage of the of laboratory work, this may lead to higher differential pressure or pressure drawdown across the formation which is greater than the formation strength (UCS) can withstand; and thus may lead to failure and breakdown of the sand fabric.



- Possible chemical reaction between the SI specie and grain cement leading to cement disintegration or weakening. This may lead to the weakening of grain fabrics and subsequent sand failure and breakdown.
- Possible alteration of the formation grain interfacial tension by the injected inhibitor specie which may lead to the breakdown of the cohesive strength furnished by capillary bonding due to reduced capillary bonding between the formation grains.

### **Conclusions**

Laboratory evidence provided in this work suggests that application of scale inhibitor can have detrimental effects on the reservoir formation which may lead to physically and chemically-induced failure; and release and production of sand with the fluid streams. In addition, conceptual physico-chemical failure models for analyzing and explaining inhibitor-formation interaction are proposed. However, further numerical and laboratory work using analytical methods are recommended to confirm the proposed physico-chemical models.

### **References**

Engebretson, R. R., Von Wandruszka, R., Seto, M., Nag, D. K., Vutukuri, V. S. and Katsuyama, K. (1997). Effect of Chemical Additives on the Strength of Sandstone. *International Journ. of Rock Mech. & Min. Sc. & Geomech. Abs.*, vol 34, no 3, April; pp. 691.

Graham, G. M., Oluyemi, G and Stalker, R. (2009). Modelling Staged Diversion Treatments and Chemical Placement in the Presence of Near-wellbore Fractures. SPE Int. Symp. On Oilfield Chemistry, 20-22 April 2009; Woodlands, Texas; USA.

Han, G. and Dusseault, M. B. (2002). Quantitative Analysis of Mechanism for Water-Related Sand Production. SPE 73737, Inter. Symp. & Exihib. On Formation Damage Control; Lafayette, Louisiana; Feb. 20-21.

Han G., Dusseault, M.B., Cook, J. (2002). Quantifying Rock Capillary Strength Behaviour in Unconsolidated Sandstones. SPE/ISRM 78170, SPE/ISRM Rock Mechanics Conference, Irving, Texas, October 20-23.

Oluyemi, G. (2007). Intelligent Grain Size Profiling Using Neural Network and Application to Sanding Potential Prediction in Real Time. PhD Thesis, The Robert Gordon University, November; Aberdeen, UK.

Oluyemi, G., Oyeneyin, M.B. & Macleod, C., (2010). UCS Neural Network Model for Real Time Sand Prediction. International Journal of Engineering Research in Africa, Vol. 2; pp 1-13.

Oluyemi, G., Stalker, R., Graham, G. M. (2009). Chemical Placement in Fractured Systems: Laboratory Characterisation and Evaluation of Fractured Cores. 20<sup>th</sup> Int. Oilfield Chemistry Symposium, March 22-25; Geilo, Norway.

Papamichos E., Brignoli M and Santarelli F J, (1997). An Experimental and Theoretical Study of a Partially Saturated Collapsible Rocks. *Mechanics of Cohesive-Frictional Materials*, 2, pp 1-28.

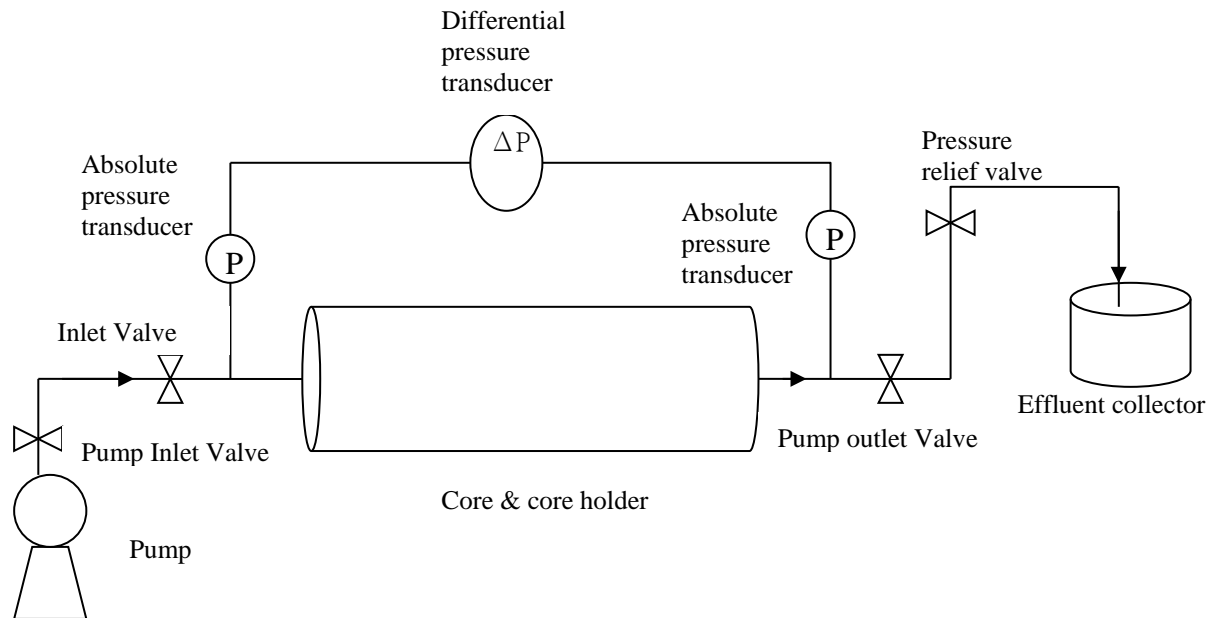


Figure 1 - Process design layout of the coreflood rig set-up

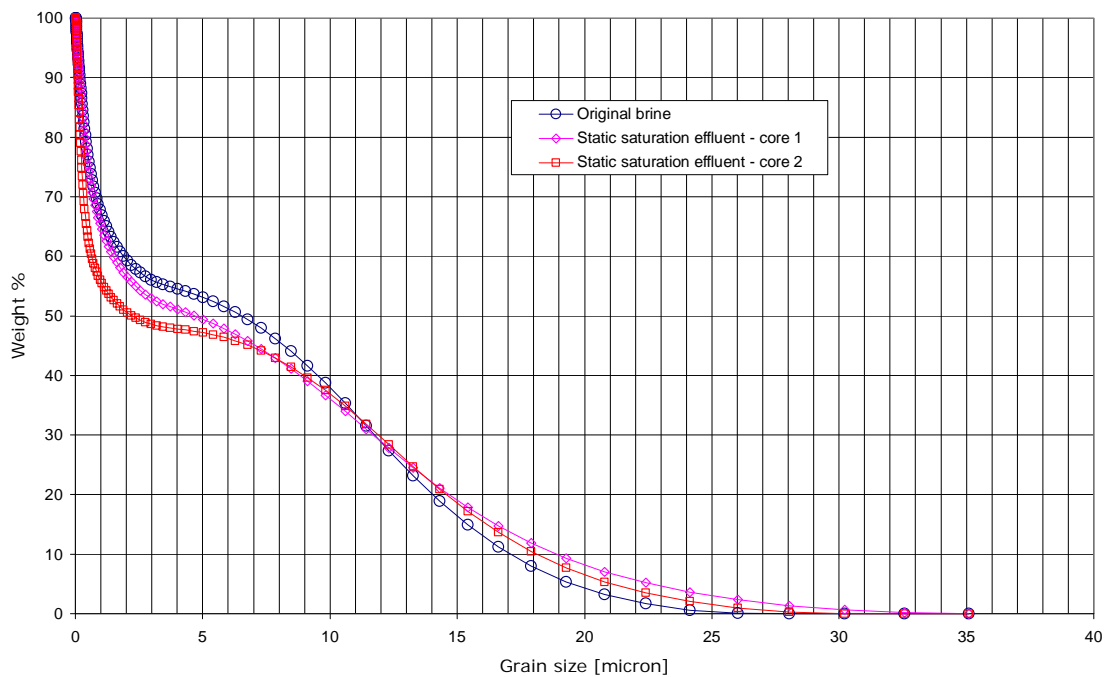


Figure 2 - Static brine saturation – comparison of grain size distributions of the original brine and brine effluents from Cores 1 and 2

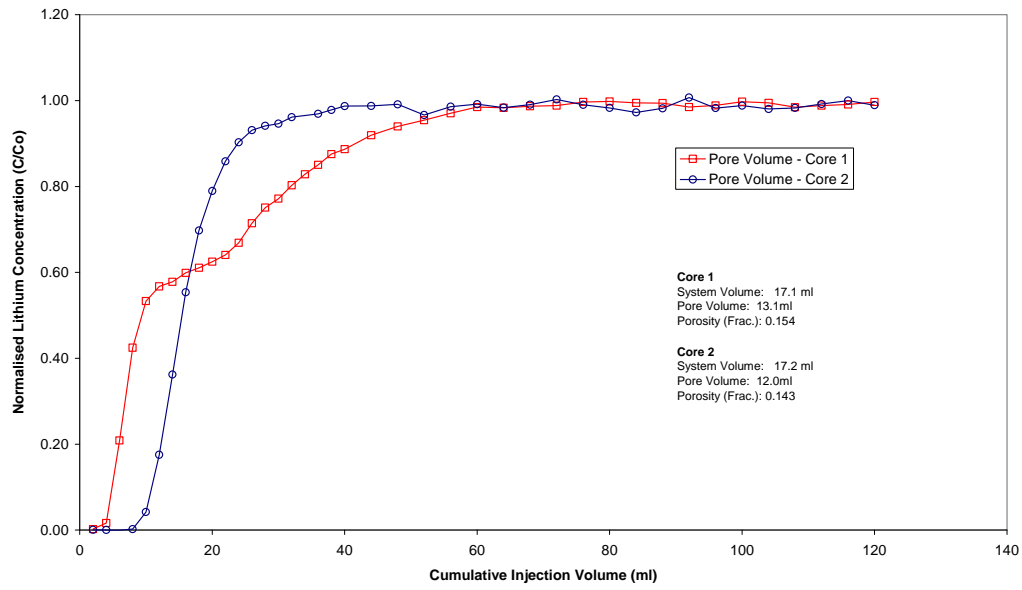


Figure 3 - Li tracer profiles obtained from the pore volume and porosity measurements of Cores 1 and 2

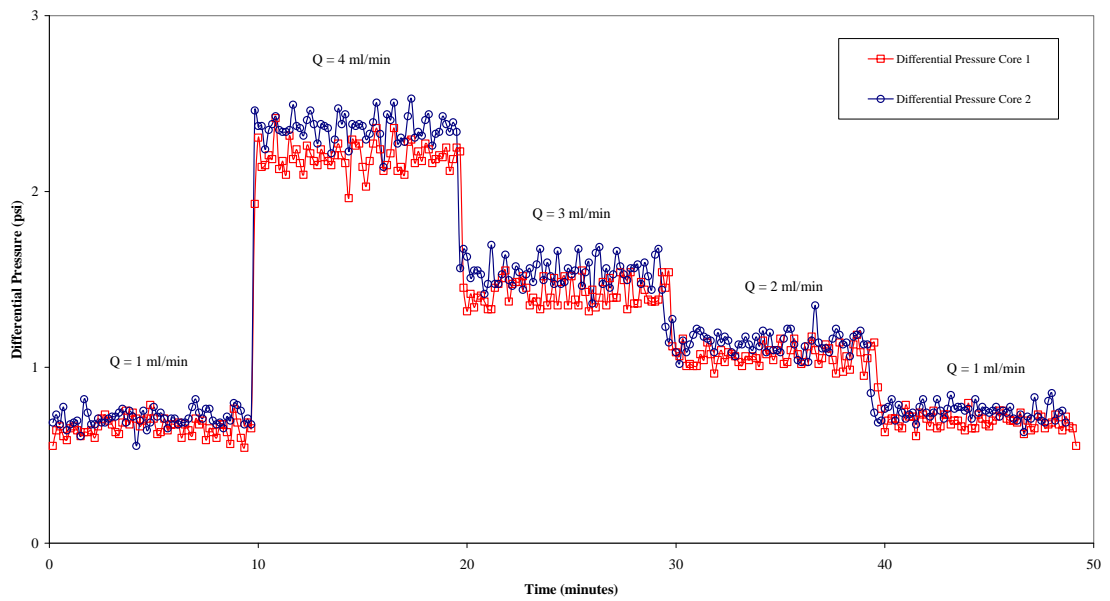


Figure 4 - Pressure profiles obtained from the permeability measurements for Cores 1 and 2

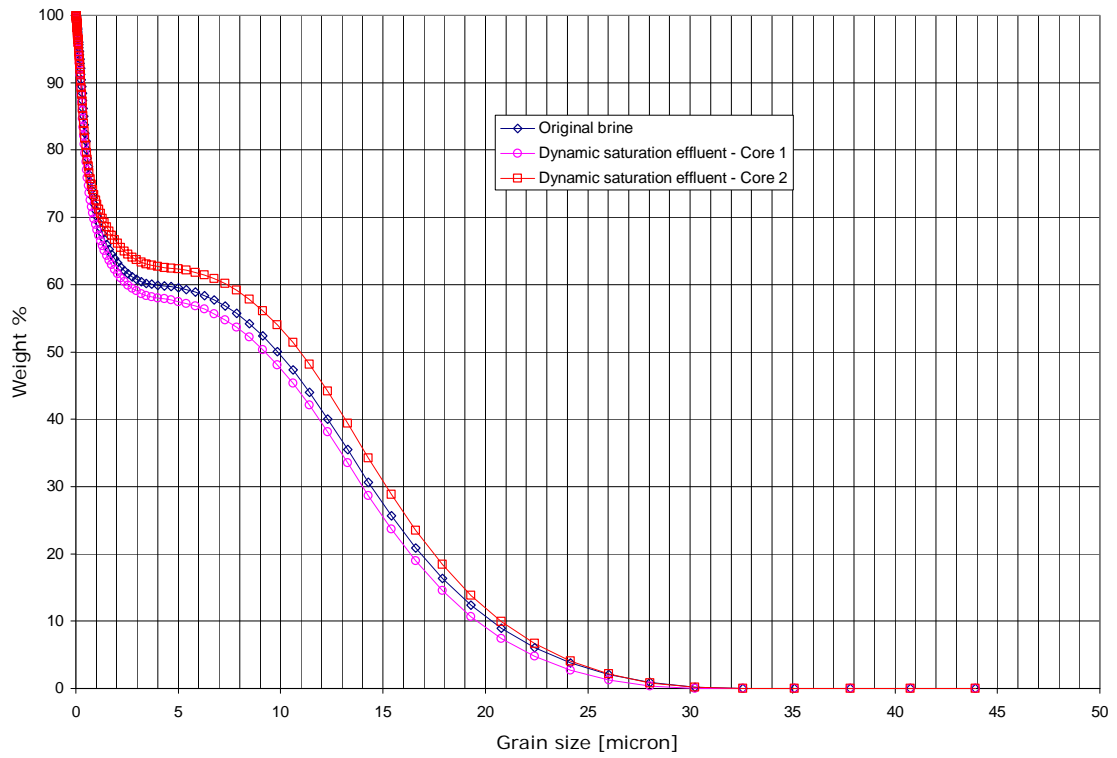


Figure 5 - Dynamic brine saturation – comparison of grain size distributions of the original brine and brine effluents from Cores 1 and 2

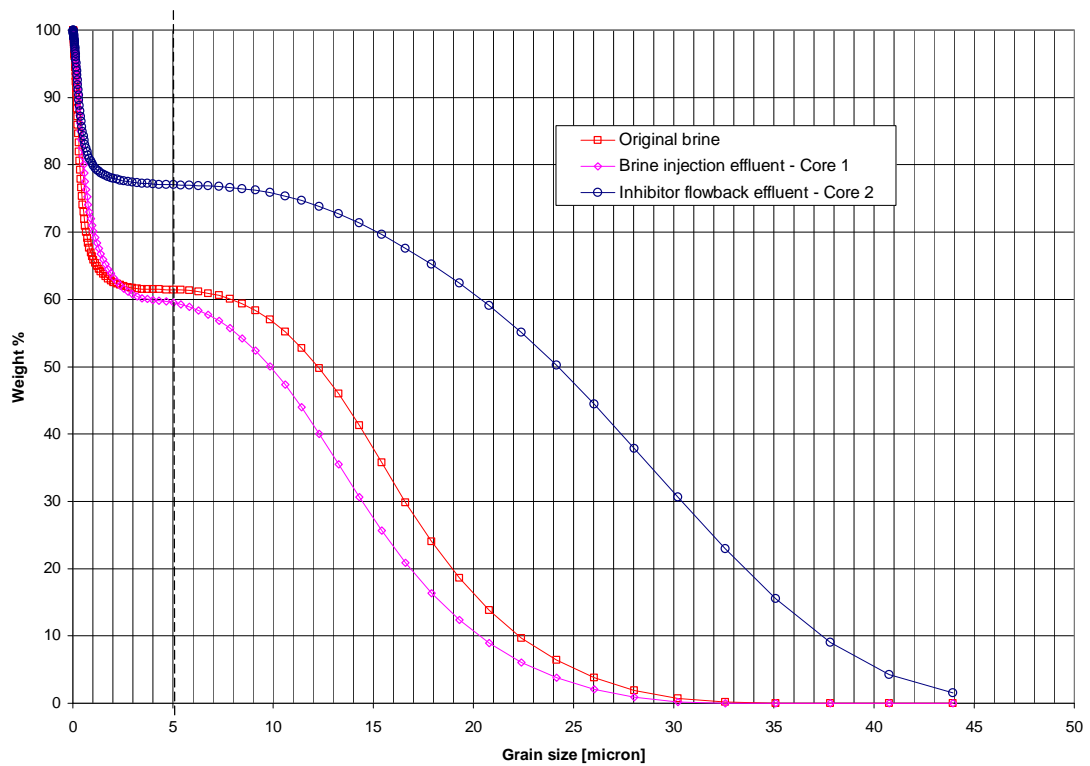


Figure 6 - Dynamic Inhibitor injection – comparison of grain size distributions of the original brine and SI effluents from Cores 1 and 2

Table 1 - Core dimensions

|        | Length [cm] | Diameter [cm] | Cross-sectional area [cm <sup>2</sup> ] |
|--------|-------------|---------------|---|
| Core A | 7.55        | 3.8           | 11.3                                    |
| Core B | 7.45        | 3.81          | 11.39                                   |

Table 2 - Brine composition

| Salt                                  | Concentration [ppm] |
|---------------------------------------|---------------------|
| NaCl                                  | 10392               |
| CaCl <sub>2</sub> .2.H <sub>2</sub> O | 426                 |
| MgCl <sub>2</sub> .6H <sub>2</sub> O  | 630                 |
| KCl                                   | 208                 |
| SrCl.6H <sub>2</sub> O                | 10                  |

Table 3 - Core pore volume and porosity

|        | Porosity [frac] | Pore volume [ml] | Permeability [mD] |
|--------|-----------------|------------------|-------------------|
| Core A | 17.3            | 17.1             | 83                |
| Core B | 0.143           | 0.154            | 77                |

Table 4 - Core permeability

|        | dq/dp gradient | Permeability [mD] |
|--------|----------------|-------------------|
| Core A | 0.12375        | 83                |
| Core B | 0.11515        | 77                |